

Short term unpredictability of high Reynolds number turbulence — rough dependence on initial data

Z. C. Feng and Y. Charles Li

ABSTRACT. Short term unpredictability is discovered numerically for high Reynolds number fluid flows under periodic boundary conditions. Furthermore, the abundance of the short term unpredictability is also discovered. These discoveries support our theory that fully developed turbulence is constantly driven by such short term unpredictability.

1. Introduction

Turbulence as an open problem has two aspects: turbulence engineering and turbulence physics [10]. Turbulence engineering deals with how to describe turbulence in engineering. Turbulence physics deals with the physical mechanism of turbulence. In pursuit of understanding of turbulence physics, recently we proposed the theory that fully developed turbulence is caused by short term unpredictability due to rough dependence upon initial data, while (often) transient turbulence at moderate Reynolds number is caused by chaos (long term unpredictability) [11]. The main goal of this article is to demonstrate the short term unpredictability via numerical simulations. According to our analytical theory [11], perturbations in turbulence can amplify in time according to $e^{\sigma\sqrt{Re}\sqrt{t}+\sigma_1 t}$ where $\sigma_1 = \frac{\sqrt{2e}}{2}\sigma$ and σ depends only on the base solutions on which the perturbations are introduced. When the time is small, the first term in the exponent dominates, and this term can cause the amplification to be superfast when the Reynolds number is large. By the time $t \sim Re$, the two terms in the exponent are about equal. After the time $t \sim Re$, the second term dominates, and this term is the classical Liapunov exponent that causes chaos (long term unpredictability). Thus the time $t \sim Re$ is the temporal separation point between short term unpredictability and long term unpredictability. When the Reynolds number is large, long before the separation point $t \sim Re$, the first term in the exponent already amplifies the perturbation to substantial size, and the second term does not get a chance to act. Thus fully developed turbulence is dominated by such short term unpredictability. When the

1991 *Mathematics Subject Classification.* PACS: 47.10.-g; 47.27.-i.

Key words and phrases. Short term unpredictability, rough dependence on initial data, turbulence, chaos, sensitive dependence on initial data.

Reynolds number is moderate, both terms in the exponent have a chance to dominate, and the corresponding (often) transient turbulence is dominated by chaos in long term.

Long term unpredictability has been well understood. The main feature of chaos is long term unpredictability led by sensitive dependence on initial data. On the other hand, short term unpredictability is led by rough dependence on initial data. If the solutions are non-differentiable in their initial data, as in the case of Euler equations of fluids [3], then any small initial perturbation will be amplified to order $O(1)$ instantly. Such a short term unpredictability is very different from the long term unpredictability of chaos. Such a short term unpredictability is closer to total randomness than the long term unpredictability of chaos. Nevertheless, such a short term unpredictability is still not total randomness, for instance the solutions of Euler equations of fluids are still continuous in their initial data. Such a short term unpredictability leads to a peculiar process that is very close to a random process but still constrained. When the Reynolds number is moderate, dynamics of Navier-Stokes equations is quite far away from that of Euler equations. Turbulence at such a stage is often transient, and bears clear resemblance to finite dimensional chaos [15] [8] [2] [14] [1] [16] [7] [6]. One can name such turbulence as chaos in Navier-stokes equations. Such turbulent solutions are differentiable in their initial data (at least during the known time interval of existence), and the derivatives of the solutions in initial data have moderate norms. When the Reynolds number is very high, dynamics of Navier-Stokes equations is getting closer to that of Euler equations. High Reynolds number turbulence is fully developed, and has no resemblance to finite dimensional chaos. Such turbulent solutions are still differentiable in their initial data (at least during the known time interval of existence), but the derivatives of the solutions in initial data have huge norms in the order of $e^{\sigma\sqrt{Re}\sqrt{t}+\sigma_1 t}$ mentioned above which represent the growth rate of the perturbations. Thus initial perturbations are amplified super fast even in short time. We believe that this causes the abrupt nature in the development of high Reynolds number turbulence. Since perturbations constantly exist, there are constantly such super fast amplifications of perturbations which lead to the persistence nature of high Reynolds number turbulence (so-called fully developed turbulence) in contrast to the transient nature of moderate Reynolds number turbulence.

In terms of phase space dynamics of dynamical systems, when the Reynolds number is very high, fully developed turbulence is not the result of a strange attractor, rather a result of super fast amplifications of ever present perturbations. Strange attractor is a long time object, while the development of such violent turbulence is of short time. Such fully developed turbulence is maintained by constantly super fast perturbation amplifications. When the Reynolds number is set to infinity, the perturbation amplification rate is infinity. So the dynamics of Euler equations is very close to a random process. In contrast, chaos in finite dimensional conservative systems often manifests itself as the so-called stochastic layers. Dynamics inside the stochastic layers has the long term sensitive dependence on initial data. When the Reynolds number is moderate, viscous diffusive term in Navier-Stokes equations is stronger, perturbation amplification rate is moderate. At this stage, turbulence is basically chaos in Navier-Stokes equations [15] [8] [2] [14] [1] [16] [7] [6]. In some cases, strange attractor can be observed [15].

The article is organized as follows: In section 2, we briefly review Liapunov exponent and chaos. In section 3, we briefly review analytical results on rough dependence. In section 4, we are going to shed new light on the classical hydrodynamic instability theory from a new perspective. In section 5, 2D numerical demonstration on rough dependence is presented. In section 6, 3D numerical demonstration on rough dependence is presented. Section 7 is the conclusion.

2. Chaos — sensitive dependence on initial data

There are many ways to characterize chaos, and one necessary ingredient of every characterization is “sensitive dependence on initial data”. For solutions that exhibit sensitive dependence on initial data, their initial small perturbations are usually amplified exponentially (with an exponent named Liapunov exponent), and it takes time for the perturbations to accumulate to substantial amount (say order $O(1)$ relative to the small initial perturbations). If ϵ is the initial small perturbation, and σ is the Liapunov exponent, then the time for the perturbation to reach order $O(1)$ is about

$$\frac{1}{\sigma} \ln \frac{1}{\epsilon}.$$

The Liapunov exponent σ is a long term object defined by

$$\sigma = \lim_{t \rightarrow +\infty} \lim_{\delta u_0 \rightarrow 0} \frac{1}{t} \ln \frac{\|\delta u(t)\|}{\|\delta u_0\|},$$

where δu_0 is the initial perturbation, and $\|\cdot\|$ is certain norm. Positive Liapunov exponent usually is a good indicator of chaos (even though the matter can be tricky sometimes [9]). In the phase space of the dynamics, when the Liapunov exponent is positive, initially nearby orbits diverge exponentially with the exponential rate being the Liapunov exponent. If these orbits are bounded in the phase space, then it is intuitively natural to expect the dynamics being chaotic.

There are of course other ways for solutions of deterministic systems to be “irregular” than that of chaotic solutions. Next we will describe another way: rough dependence on initial data.

3. High Reynolds number turbulence — rough dependence on initial data

Turbulent motion of fluids is quite accurately modeled by the so-called Navier-Stokes equations. The phase space of the dynamics of Navier-Stokes equations has to be infinite dimensional. The well known such a phase space is the Sobolev space of divergence free fields, $H^n(\mathbb{R}^d)$ ($d = 2, 3$) which contains functions that are square-integrable and so are their derivatives up to n -th order. When $n > \frac{d}{2} + 1$ ($d = 2, 3$), for any initial condition in such a phase space, it is known [4] [5] that there is a (short) time $T > 0$ depending on the norm of the initial condition, such that the corresponding solution (orbit) of Navier-Stokes equations (and Euler equations) exists on $[0, T]$. Such an orbit is continuous in time t and its initial condition. As $Re \rightarrow \infty$, the solution of Navier-Stokes equations converges to that of the Euler equation. In 2 dimensions ($d = 2$), the existence time T is infinite, while in 3 dimensions ($d = 3$), global existence is still an open problem. The above claims apply also to spatially periodic domain \mathbb{T}^d in stead of \mathbb{R}^d .

One can define a solution map inside the phase space by mapping the initial condition to the solution's value at time t . The solution map for Euler equations ($d = 2, 3$) is continuous, but nowhere uniformly continuous, and more importantly nowhere differentiable [3]. Then it is natural to expect that the norm of the derivative of the solution map for Navier-Stokes equations approaches infinity everywhere as the Reynolds number approaches infinity. Under Euler dynamics, any small perturbation of the initial condition can potentially reach substantial amount instantly. It is natural to expect that under high Reynolds number Navier-Stokes dynamics, small perturbation of the initial condition can potentially reach substantial amount in a very short time (the larger Reynolds number, the shorter). We call this phenomenon "rough dependence on initial data". Such rough dependence on initial data naturally leads to the violent fully developed turbulence as observed in experiments. One can try to estimate the size of the derivative of the solution map for Navier-Stokes equations. The Navier-Stokes equations are given by

$$(3.1) \quad u_t - \frac{1}{Re} \Delta u = -\nabla p - u \cdot \nabla u,$$

$$(3.2) \quad \nabla \cdot u = 0,$$

where u is the d -dimensional fluid velocity ($d = 2, 3$), p is the fluid pressure, and Re is the Reynolds number. Setting the Reynolds number to infinity $Re = \infty$, the Navier-Stokes equations (3.1) reduces to the Euler equations

$$(3.3) \quad u_t = -\nabla p - u \cdot \nabla u,$$

$$(3.4) \quad \nabla \cdot u = 0.$$

For any $u \in H^n(\mathbb{R}^d)$, there is a neighborhood B and a short time $T > 0$, such that for any $v \in B$ there exists a unique solution to the Navier-Stokes equations (3.1) in $C^0([0, T]; H^n(\mathbb{R}^d))$; as $Re \rightarrow \infty$, this solution converges to that of the Euler equations (3.3) in the same space. For any $t \in [0, T]$, let S^t be the solution map:

$$(3.5) \quad S^t : B \mapsto H^n(\mathbb{R}^d), \quad S^t(u(0)) = u(t),$$

i.e. the solution map maps the initial condition to the solution's value at time t . The solution map is continuous for both Navier-Stokes equations (3.1) and Euler equations (3.3) [4] [5]. A recent result of Inci [3] shows that for Euler equations (3.3) the solution map is nowhere differentiable. Even though the derivative of the solution map for Navier-Stokes equations (3.1) exists, it is natural to conjecture that the norm of the derivative of the solution map approaches infinity everywhere as the Reynolds number approaches infinity. The following upper bound was obtained in [11].

$$(3.6) \quad \|DS^t(u(0))\| = \sup_{\delta u(0)} \frac{\|\delta u(t)\|}{\|\delta u(0)\|} \leq e^{\sigma \sqrt{Re} \sqrt{t} + \sigma_1 t},$$

where $\delta u(0)$ is any initial perturbation of $u(0)$, and

$$\sigma = \frac{8}{\sqrt{2e}} \max_{\tau \in [0, T]} \|u(\tau)\|_n, \quad \sigma_1 = \frac{\sqrt{2e}}{2} \sigma.$$

The above bound also applies to spatially periodic domain \mathbb{T}^d in stead of \mathbb{R}^d . The main aim of this article is to numerically demonstrate that in fully developed turbulence, perturbations amplify according to the growth rate given by the right hand side of (3.6).

4. Classical hydrodynamic instability — directional derivative

Classical hydrodynamic instability theory mainly focuses on the so-called linear instability of steady fluid flows. We can think that the linear instability theory is based on Taylor expansion of the solution map for Navier-Stokes equations (3.1). Let u^* be the steady flow (a fixed point in the phase space), v_0 be its initial perturbation, and $u^* + v(t)$ be the solution to the Navier-Stokes equations (3.1) with the initial condition $u^* + v_0$. According to Taylor expansion,

$$v(t) = dv(t) + d^2v(t) + \cdots,$$

where $dv(t)$ is the first differential in $u^* + v_0$ of the solution map at the steady flow u^* , similarly for $d^2v(t)$ etc.. Under the Euler dynamics, this expansion fails since the first differential does not exist [3]. Under the Navier-Stokes dynamics, this expansion is valid, and the first differential satisfies the differential form

$$(4.1) \quad dv_t - \frac{1}{Re} \Delta dv = -\nabla dp - dv \cdot \nabla u^* - u^* \cdot \nabla dv,$$

$$(4.2) \quad \nabla \cdot dv = 0,$$

where dp is the pressure differential. The linear instability refers to the instability of the differential form (4.1). In most cases studied, the steady flow u^* depends on only one spatial variable y (the so-called channel flow). This permits the following type solutions to the differential form,

$$(4.3) \quad dv(t) = \exp\{i(\sigma t + k_1 x + k_3 z)\} V(y),$$

where (x, y, z) are the spatial coordinates, σ is a complex parameter, and (k_1, k_3) are real parameters. One can view (4.3) as a single Fourier mode out of the Fourier transform of $dv(t)$. In the phase space of the dynamics, (4.3) is a directional differential with the specific direction specified by the (k_1, k_3) Fourier mode. $V(y)$ satisfies the well-known Orr-Sommerfeld equation (Rayleigh equation in the inviscid case $Re = \infty$). Even though the first differential $dv(t)$ does not exist in the inviscid case ((4.1) with $Re = \infty$), the directional differential (4.3) can exist with $V(y)$ solving the Rayleigh equation. Thus, the linear stability/instability predicted by the Rayleigh equation only represents a directional linear stability/instability of the Euler dynamics while the full first differential of the Euler dynamics does not exist. The classical hydrodynamic instability theory heavily focuses on the studies of the Rayleigh equation. Such a study is still important since the directional linear instability derived from Rayleigh equation often imply linear instability in Orr-Sommerfeld equation [13]. The linear instability of the Orr-Sommerfeld equation indeed represents the linear instability of the full first differential of the Navier-Stokes equations.

5. 2D numerical simulations on rough dependence on initial data

5.1. A fundamental problem in the numerical simulations. First we numerically simulate an explicit example [12] to test the numerical performance. Consider the 2D Navier-Stokes equations

$$(5.1) \quad \partial_t u + u \cdot \nabla u = -\nabla p + \frac{1}{Re} \Delta u, \quad \nabla \cdot u = 0,$$

under periodic boundary condition with period domain $[0, 2\pi] \times [0, 2\pi]$, where $u = (u_1, u_2)$ is the velocity, p is pressure, and the spatial coordinate is denoted by

$x = (x_1, x_2)$. A simple solution to the 2D Navier-Stokes equations (5.1) is

$$(5.2) \quad u_1 = \sum_{n=1}^{\infty} \frac{1}{n^{3+\gamma}} e^{-\frac{n^2}{Re}t} \sin[n(x_2 - \sigma t)], \quad u_2 = \sigma,$$

where $\frac{1}{2} < \gamma \leq 1$, and σ is a real parameter. By varying σ , we get a variation direction of the initial condition,

$$du_1(0) = 0, \quad du_2(0) = d\sigma,$$

which leads to the variation of the solution $(du_1(t), du_2(t))$. Let

$$\Lambda = \|(du_1(t), du_2(t))\|_{H^3}, \quad \Lambda_0 = \|(du_1(0), du_2(0))\|_{H^3},$$

then one has the analytical result [12]:

$$(5.3) \quad \frac{\Lambda}{\Lambda_0} \geq \left(1 + \left[\frac{1}{\sqrt{2e}} t^\gamma \left(\frac{\sqrt{t}\sqrt{Re}}{2\sqrt{2}} \right)^{1-\gamma} \right]^2 \right)^{1/2}.$$

This lower bound is obtained by keeping only the fastest growing mode given by

$$(5.4) \quad n = \left\lceil \sqrt{\frac{Re}{2t}} \right\rceil, \quad \left(\text{the integer part of } \sqrt{\frac{Re}{2t}} \right).$$

Notice that as $t \rightarrow 0^+$, the time derivative of the lower bound approaches positive infinity due to the fractional power of t . That is, the lower bound curve is tangent to the vertical axis at $t = 0$. As $t \rightarrow 0^+$, the fastest growing mode (5.4) $n \rightarrow +\infty$. Thus a numerical simulation will never capture the fastest growing mode as $t \rightarrow 0^+$ no matter how many Fourier modes are kept in the numerical simulation. This demonstrates a fundamental problem in numerical simulations. When we numerically simulate the quantity $\frac{\Lambda}{\Lambda_0}$ (5.3), we obtained the solid curve in Figure 2. Notice that as $t \rightarrow 0^+$, the numerical solid curve gets below the dash lower bound curve (violating the lower bound nature). The numerical solid curve has a finite time derivation at $t = 0$, and does not capture the infinite derivative nature at $t = 0$.

5.2. Fixed base solution and different perturbations. We will numerically simulate the 2D Navier-Stokes equations under periodic boundary condition (5.1). For the base solution, we choose the initial condition

$$(5.5) \quad u_1(0) = -8 \sin(9x_1) \sin(8x_2), u_2(0) = -9 \cos(9x_1) \cos(8x_2),$$

Starting from this initial condition, we solve (5.1) numerically to generate the base solution. The perturbation du based upon a base solution u solves the linearized 2D Navier-Stokes equations,

$$(5.6) \quad \partial_t du + u \cdot \nabla du + du \cdot \nabla u = -\nabla dp + \frac{1}{Re} \Delta du, \quad \nabla \cdot du = 0,$$

under the same periodic boundary condition as in (5.1). Since (5.6) is linear, we can choose single Fourier modes for the initial conditions of the perturbations,

$$(5.7) \quad du_1(0) = -0.1k_2 \sin(k_1x_1) \sin(k_2x_2), du_2(0) = -0.1k_1 \cos(k_1x_1) \cos(k_2x_2).$$

Figure 2 shows the super fast growth of the perturbation when

$$(5.8) \quad k_1 = 1, k_2 = 1, Re = 1000 \text{ and } Re = 100000,$$

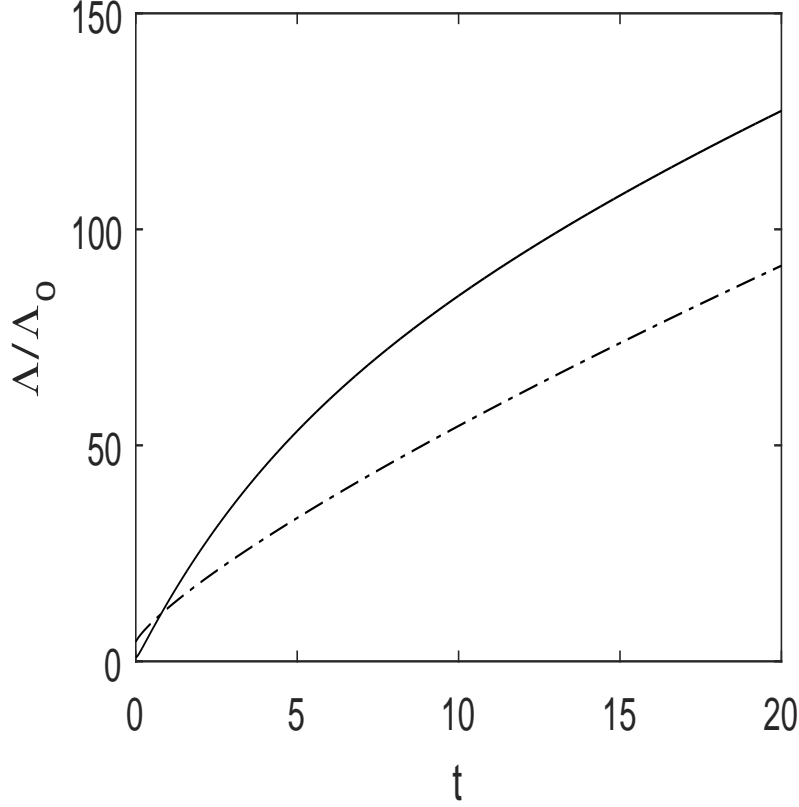


FIGURE 1. This figure clearly illustrates the fundamental obstacle in numerical simulation on the norm of the solution map's derivative as $t \rightarrow 0^+$. The dash curve represents the analytically obtained lower bound (5.3) on the norm of the directional derivative of a family of explicit solutions, where $\gamma = 0.6$ and $\sigma = 27.5$ are chosen. The solid curve represents the numerical simulation on the norm of the directional derivative of the same family of explicit solutions. One can see clearly that near $t = 0$, the rigorous lower bound is violated. In particular, the dash curve has infinite derivative at $t = 0$, while the solid curve has finite derivative.

where the time step for the numerical simulation is $\Delta t = 0.0005$. We use the notation that

$$(5.9) \quad \Lambda(t) = \|du(t)\|_{H^3}.$$

Then the norm of the derivative of the solution map at the base solution $u(t)$ is given by

$$(5.10) \quad \|DS^t(u(0))\| = \sup_{du(0)} \frac{\Lambda(t)}{\Lambda(0)}.$$

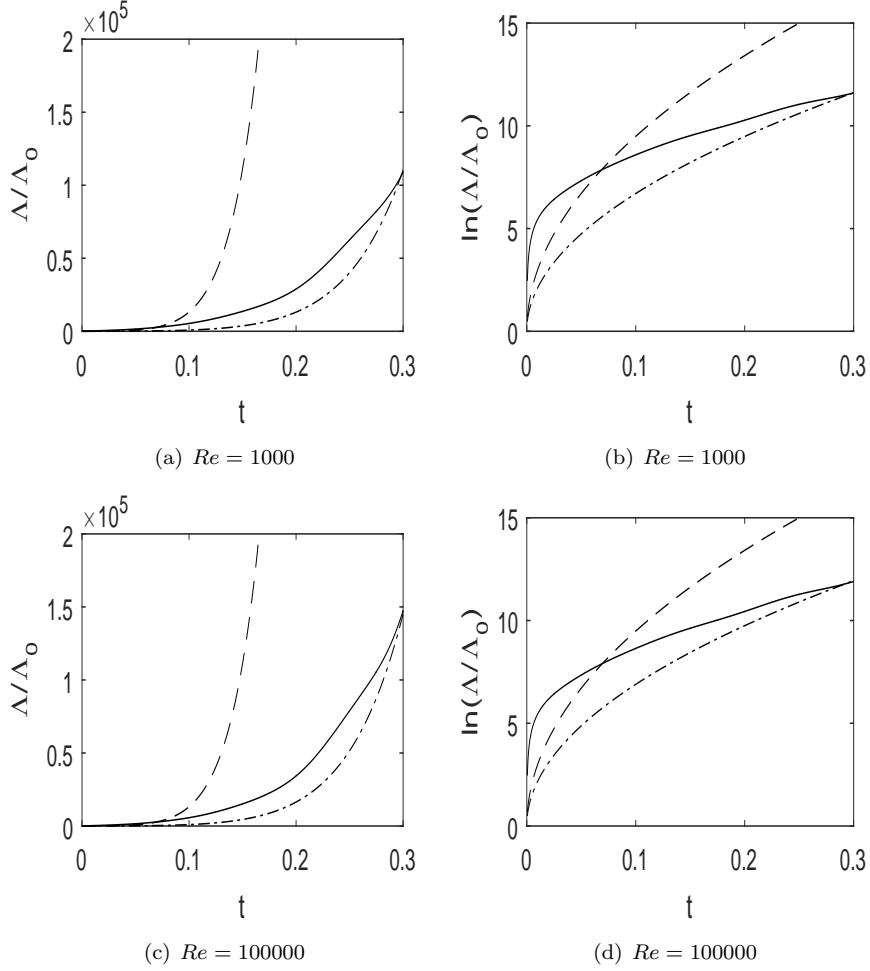


FIGURE 2. The solid curve is the numerical result of the super fast growth of perturbations with initial condition (5.7)-(5.8) where $\Lambda(t) = \|du(t)\|_{H^3}$. The lower fitting dashed curve is $e^{21.2\sqrt{t}}$ when $Re = 1000$ and $e^{21.7\sqrt{t}}$ when $Re = 100000$. The closest fitting dashed curve is $e^{30\sqrt{t}}$ when $Re = 1000$ and $Re = 100000$.

Notice that for any fixed t , the supremum is taken with respect to all initial perturbation $du(0)$. If one initial perturbation leads to a perturbation that is near the supremum for some t , it may not be near the supremum for other t . The norm of the derivative $\|DS^t(u(0))\|$ has an upper bound given by (3.6). The growth of the perturbation in Figure 2 realizes the nature of the square root of time in the exponent of (3.6). The nature of the square root of the Reynolds number in the exponent of (3.6) is not realized by the particular perturbation since the viscous effect is negligible in both cases $Re = 1000$ and $Re = 100000$. We believe that the nature of the square root of the Reynolds number in the exponent of (3.6) can only

be realized by all the perturbations. For any particular perturbation, the viscous effect is negligible when the Reynolds number is relatively large. Increasing the wave number (k_1, k_2) , the perturbation's growth rate decreases as shown in Figures 3 - 4. When the wave number of the initial perturbation is larger, the viscous effect is more significant. Our conclusion is that the super fast growth (rough dependence) is abundant among perturbations in the sense that generic perturbations contain all Fourier modes, and low Fourier modes display the super fast growth. Next we shall study the abundance of the super fast growth among base solutions, that is, whether or not there are abundant base solutions of which the perturbations have super fast growth.

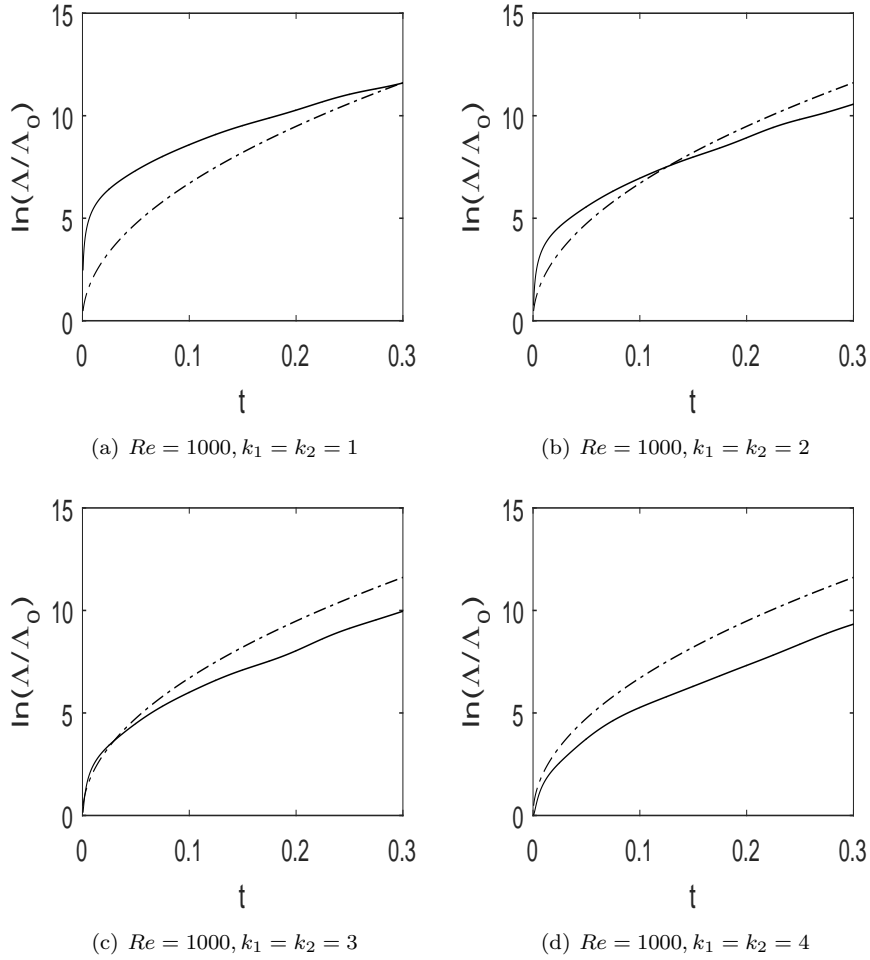


FIGURE 3. The solid curve is the numerical result of the super fast growth of perturbations with initial condition (5.7) with different (k_1, k_2) where $\Lambda(t) = \|du(t)\|_{H^3}$. The fitting dashed curve is $e^{21.2\sqrt{t}}$.

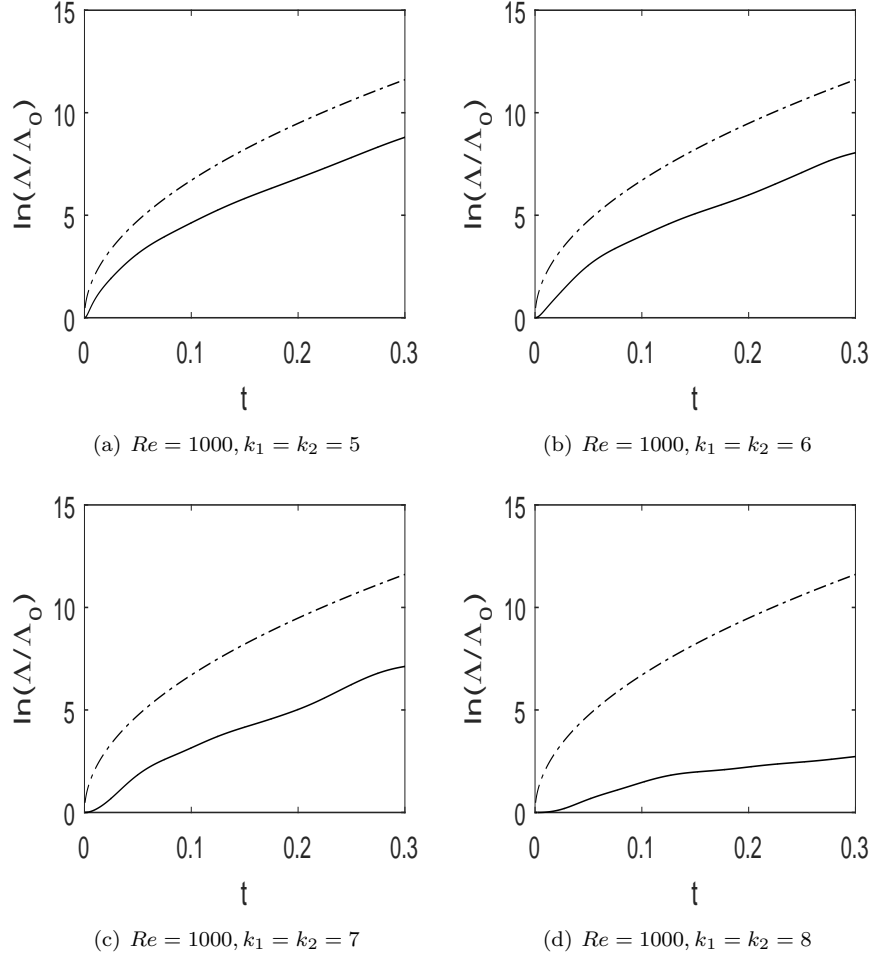


FIGURE 4. The solid curve is the numerical result of the super fast growth of perturbations with initial condition (5.7) with different (k_1, k_2) where $\Lambda(t) = \|du(t)\|_{H^3}$. The fitting dashed curve is $e^{21.2\sqrt{t}}$.

5.3. Fixed perturbation and different base solutions. First we fix the initial condition of the perturbation to be the case of $k_1 = 1$ and $k_2 = 1$ in (5.7), and the Reynolds number $Re = 1000$. Then we simulate different base solutions with initial conditions of the form,

$$(5.11) \quad u_1(0) = -k_2 \sin(k_1 x_1) \sin(k_2 x_2), \quad u_2(0) = -k_1 \cos(k_1 x_1) \cos(k_2 x_2).$$

For different choices of (k_1, k_2) , the super fast growths are shown in Figures 5-6. As the wave numbers (k_1, k_2) of the base solutions decrease, the super fast growth rates of the perturbation decrease. Together with the result of last subsection, we conclude that higher wave number base solutions and lower wave number perturbations correspond to faster super fast growth of the perturbations. Numerical

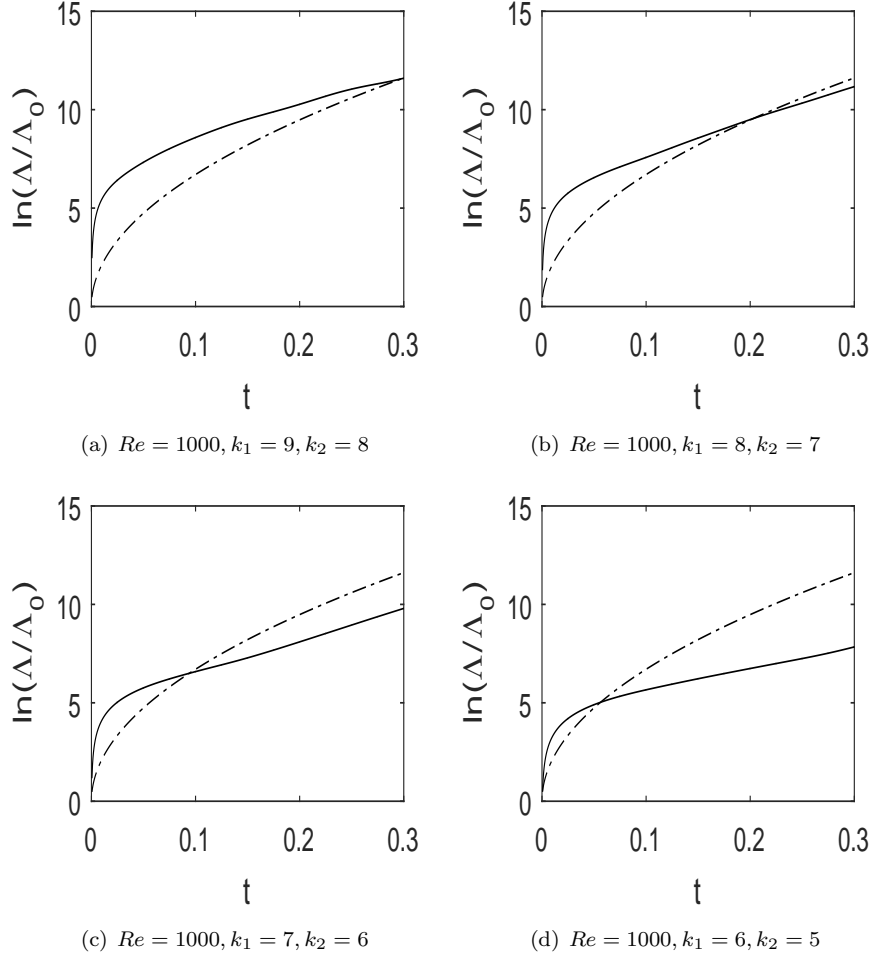


FIGURE 5. The solid curve is the numerical result of the super fast growth of perturbations with initial condition (5.7) with $k_1 = 1$ and $k_2 = 1$ under different base solutions with initial conditions given by (5.11), where $\Lambda(t) = \|du(t)\|_{H^3}$. The fitting dashed curve is $e^{21.2\sqrt{t}}$.

simulations on other base solutions also show super fast growth of the perturbations. Thus super fast growth of the perturbations (rough dependence) is also abundant among base solutions. One can then envision that when the Reynolds number is large, the super fast growth of the ever present perturbations will cause the abrupt development of turbulence, and is the mechanism that maintains the persistence of turbulence (the so called fully developed turbulence).

6. 3D numerical simulations on rough dependence on initial data

In this section, we numerically simulate the 3D Navier-Stokes equations (3.1) and the corresponding perturbation equations (the same form with (5.6)) under

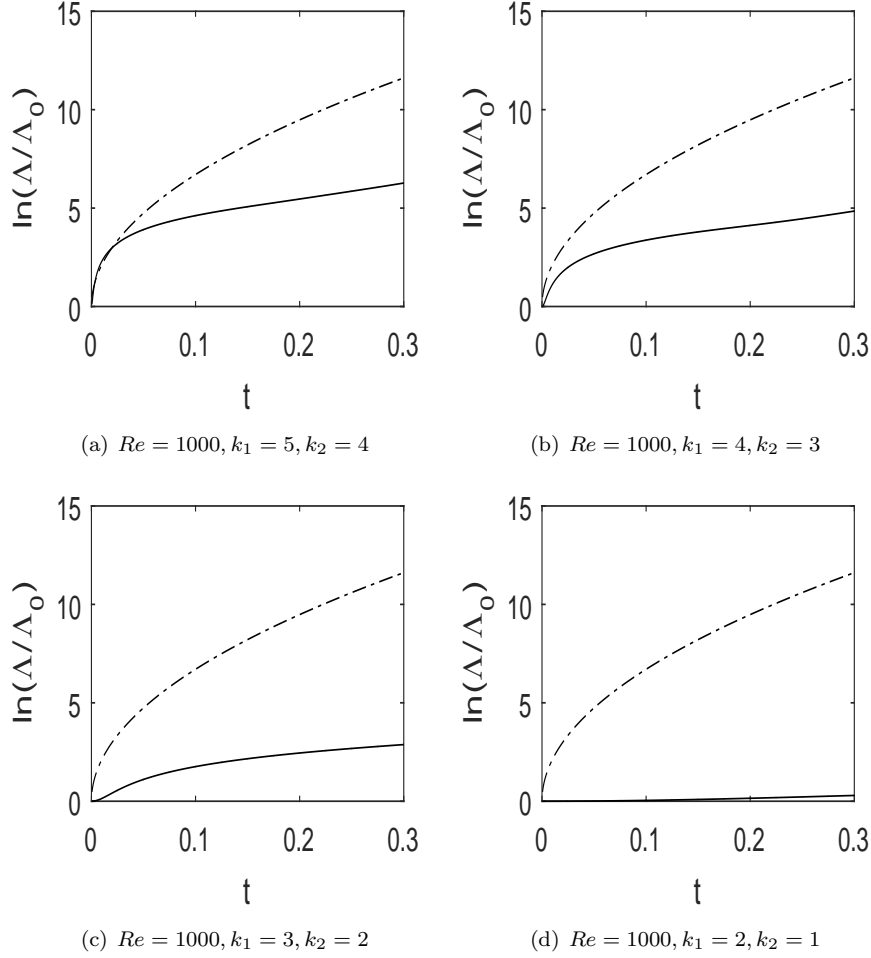


FIGURE 6. The solid curve is the numerical result of the super fast growth of perturbations with initial condition (5.7) with $k_1 = 1$ and $k_2 = 1$ under different base solutions with initial conditions given by (5.11), where $\Lambda(t) = \|du(t)\|_{H^3}$. The fitting dashed curve is $e^{21.2\sqrt{t}}$.

the periodic boundary condition with period domain $[0, 2\pi] \times [0, 2\pi] \times [0, 2\pi]$. We start with the initial condition for the base solution in the form

$$\begin{aligned}
 u_1(0) &= \frac{A}{k_1} \cos(k_1 x_1) \sin(k_2 x_2) \sin(k_3 x_3), \\
 u_2(0) &= \frac{A}{k_2} \sin(k_1 x_1) \cos(k_2 x_2) \sin(k_3 x_3), \\
 u_3(0) &= -2 \frac{A}{k_3} \sin(k_1 x_1) \sin(k_2 x_2) \cos(k_3 x_3),
 \end{aligned}
 \tag{6.1}$$

and the initial condition for the perturbation in the form

$$\begin{aligned}
 du_1(0) &= \frac{a}{\hat{k}_1} \cos(\hat{k}_1 x_1) \sin(\hat{k}_2 x_2) \sin(\hat{k}_3 x_3), \\
 du_2(0) &= \frac{a}{\hat{k}_2} \sin(\hat{k}_1 x_1) \cos(\hat{k}_2 x_2) \sin(\hat{k}_3 x_3), \\
 du_3(0) &= -2 \frac{a}{\hat{k}_3} \sin(\hat{k}_1 x_1) \sin(\hat{k}_2 x_2) \cos(\hat{k}_3 x_3).
 \end{aligned}
 \tag{6.2}$$

6.1. Fixed base solution and different perturbations. In (6.1)-(6.2), we choose

$$Re = 1000, \quad A = 20, \quad k_1 = 6, \quad k_2 = 5, \quad k_3 = 1, \quad a = 0.1,
 \tag{6.3}$$

and time step $\Delta t = 0.00025$. Figure 7 shows the super fast growth of the pertur-

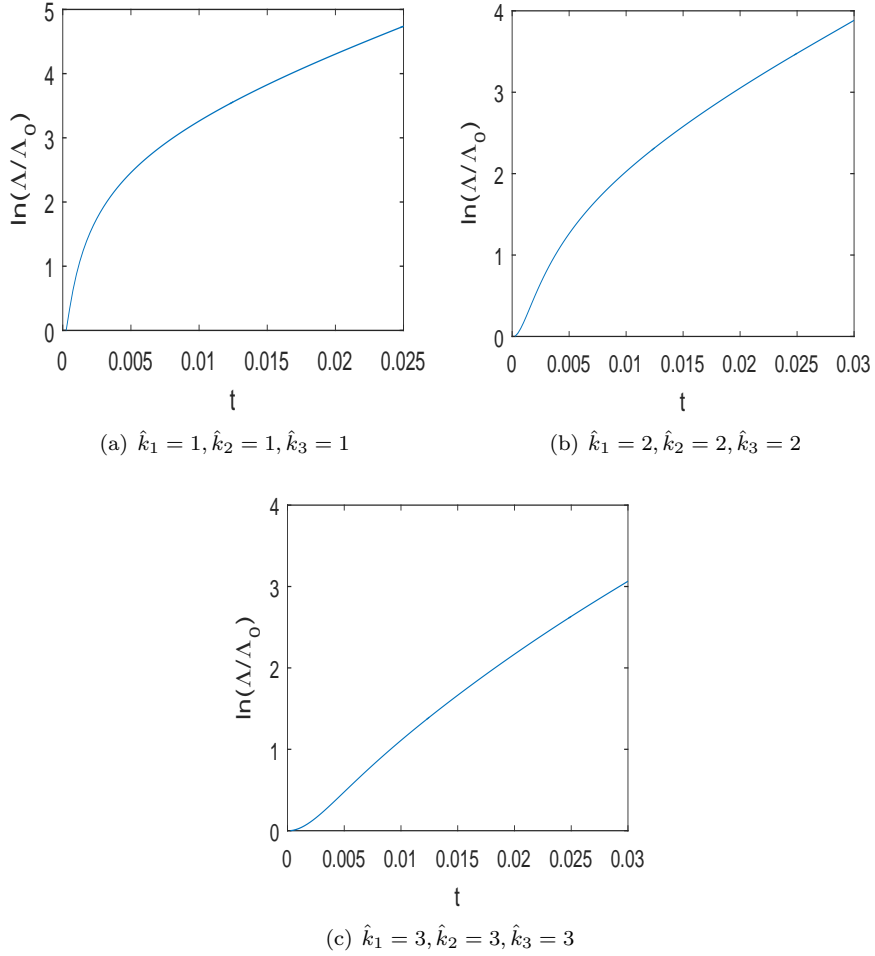


FIGURE 7. Super fast growth of the perturbations of different modes in 3D with parameters (6.3).

bations of different modes where $\Lambda(t)$ is defined in (5.9). We arrive at the same conclusion as in 2D, that is, lower wave number perturbations have faster super fast growth, and such super fast growth is abundant among perturbations.

6.2. Fixed perturbation and different base solutions. In (6.1)-(6.2), we choose

$$(6.4) \quad Re = 1000, A = 20, \hat{k}_1 = 1, \hat{k}_2 = 1, \hat{k}_3 = 1, a = 0.1,$$

and time step $\Delta t = 0.00025$. Figure 8 shows the super fast growth of the perturba-

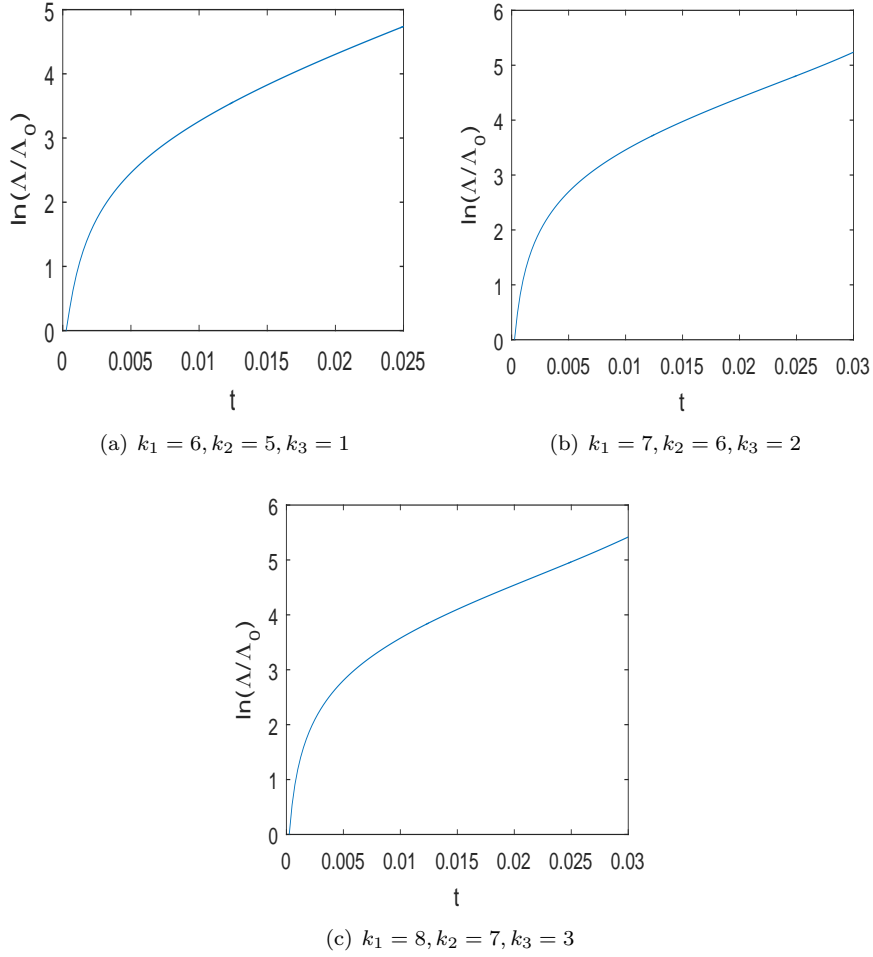


FIGURE 8. Super fast growth of the perturbation under different base solutions in 3D with parameters (6.4).

tion under different base solutions with initial conditions of the form (6.1), where $\Lambda(t)$ is defined in (5.9). We arrive at the same conclusion as in 2D, that is, the perturbation of higher mode base solutions has faster super fast growth, and such super fast growth is abundant among base solutions.

7. Conclusion

Through numerical simulations, we demonstrated the super fast growth of perturbations (rough dependence upon initial data) in high Reynolds number fluid flows. We also showed the abundance of such super fast growth among perturbations and base solutions in support of our theory that fully developed turbulence is caused and maintained by such super fast growth of perturbations.

References

- [1] Y. Duguet, P. Schlatter, D. Henningson, Formation of turbulent patterns near the onset of transition in plane Couette flow, *J. Fluid Mech.* **650** (2010), 119-129.
- [2] J. Gibson, T. Schneider, Homoclinic snaking in plane Couette flow: bending, skewing and finite-size effects, *J. Fluid Mech.* **794** (2016), 530-551.
- [3] H. Inci, On the regularity of the solution map of the incompressible Euler equation, *Dynamics of PDE* **12**, no.2 (2015), 97-113, arXiv: 1301.5997.
- [4] T. Kato, Nonstationary flows of viscous and ideal fluids in R^3 , *J. Funct. Anal.* **9** (1972), 296-305.
- [5] T. Kato, Quasi-linear equations of evolution, with applications to partial differential equations, *Lect. Notes in Math.*, Springer **448** (1975), 25-70.
- [6] G. Kawahara, S. Kida, Periodic motion embedded in plane Couette turbulence: regeneration cycle and burst, *J. Fluid Mech.* **449** (2001), 291-300.
- [7] G. Kawahara, M. Uhlmann, L. van Veen, The significance of simple invariant solutions in turbulent flows, *Ann. Rev. Fluid Mech.* **44** (2012), 203-225.
- [8] T. Kreilos, B. Eckhardt, Periodic orbits near onset of chaos in plane Couette flow, *Chaos* **22** (2012), 047505.
- [9] G. Leonov, N. Kuznetsov, Time-varying linearization and the Perron effects, *International Journal of Bifurcation and Chaos* **17**, no.4 (2007), 1079-1107.
- [10] Y. Li, Major open problems in chaos theory, turbulence and nonlinear dynamics, *Dynamics of PDE* **10**, no.4 (2013), 379-392.
- [11] Y. Li, The distinction of turbulence from chaos - rough dependence on initial data, *Electronic Journal of Differential Equations* **2014**, no. 104 (2014), 1-8.
- [12] Y. Li, Rough dependence upon initial data exemplified by explicit solutions and the effect of viscosity, *Nonlinearity* **30** (2017), 1097-1108, arXiv:1506.05498.
- [13] Y. Li, Z. Lin, A Resolution of the Sommerfeld Paradox, *SIAM J. Math. Anal.* **43**, No.4 (2011), 1923-1954.
- [14] D. Lucas, R. Kerswell, Recurrent flow analysis in spatiotemporally chaotic 2-dimensional Kolmogorov flow, *Phys. Fluids* **27** (2015), 045106.
- [15] L. van Veen, G. Kawahara, Homoclinic tangle on the edge of shear turbulence, *Phys. Rev. Lett.* **107** (2011), 114501.
- [16] D. Viswanath, Recurrent motions within plane Couette turbulence, *J. Fluid Mech.* **580** (2007), 339-358.

DEPARTMENT OF MECHANICAL AND AEROSPACE ENGINEERING, UNIVERSITY OF MISSOURI, COLUMBIA, MO 65211

E-mail address: fengf@missouri.edu

DEPARTMENT OF MATHEMATICS, UNIVERSITY OF MISSOURI, COLUMBIA, MO 65211, USA

E-mail address: liyan@missouri.edu

URL: <http://faculty.missouri.edu/~liyan>